

Journal of Materials Chemistry B

Accepted Manuscript



This is an *Accepted Manuscript*, which has been through the Royal Society of Chemistry peer review process and has been accepted for publication.

Accepted Manuscripts are published online shortly after acceptance, before technical editing, formatting and proof reading. Using this free service, authors can make their results available to the community, in citable form, before we publish the edited article. We will replace this *Accepted Manuscript* with the edited and formatted *Advance Article* as soon as it is available.

You can find more information about *Accepted Manuscripts* in the [Information for Authors](#).

Please note that technical editing may introduce minor changes to the text and/or graphics, which may alter content. The journal's standard [Terms & Conditions](#) and the [Ethical guidelines](#) still apply. In no event shall the Royal Society of Chemistry be held responsible for any errors or omissions in this *Accepted Manuscript* or any consequences arising from the use of any information it contains.



Enzyme-instructed assembly of the core of yeast prion Sup35 to form supramolecular hydrogels

Dan Yuan,^a Junfeng Shi,^a Xuewen Du,^a Yibing Huang,^b Yuan Gao,^a and Bing Xu^{*a}

Received 00th January 20xx,
Accepted 00th January 20xx

DOI: 10.1039/x0xx00000x

www.rsc.org/

Based on the self-assembly capability of the core segment (GNNQQNY) of yeast prion Sup35, we design and synthesis a series of structurally related precursors for enzymatic formation of hydrogels. We found that, with the catalysis of alkaline phosphatase, the precursor becomes a hydrogelator that self-assembles in water to form nanofibers with an average width less than ten nanometers. Interestingly, the introduction of amyloid segment into a cytotoxic precursor (N'ffyp: D-1P) is able to abrogate the cytotoxicity of the precursor, making the resulting peptide to be cell compatible. This work contributes a new insight to the use of enzyme to form cell compatible hydrogels of peptides cross- β spine.

Introduction

Being driven by supramolecular interactions (e.g., hydrogen bonding, aromatic-aromatic interactions, and charge interactions), small molecules self-assemble in water to form nanofibers to act as the networks of supramolecular hydrogels.¹⁻⁹ Due to their resemblance to extracellular matrix (ECM), supramolecular hydrogels have received considerable research attention in past decade and promise many useful applications in tissue engineering, drug delivery,¹⁰ and cancer therapy. Interestingly, Sup35, a prion-like protein in yeast, also forms fibrillar amyloids, which have served as a model system for understanding prion diseases.¹¹ Particularly, recently studies suggest that a heptapeptide residues (GNNQQNY) in Sup35 sequence, as a mimic of the Sup35 protein, exhibit the similar amyloid like properties.¹² Coincidentally, such fibrillar nanostructures biophysically and morphologically resemble to the fibrillar assemblies of supramolecular hydrogelators,¹³⁻²⁹ which are fibrillar aggregates resulted from the extensive, non-covalent intermolecular interactions of the hydrogelators in aqueous medium.³⁰

The exception ability of self-assembly of Sup35 encourages us to explore them in the context of enzyme-instructed assembly (EIA), an emerging approach that control spatiotemporal profile of supramolecular nanofibers in cellular environment,^{20, 31-40} and examine the corresponding cellular responses. Specifically, we insert the peptide segment (GNNQQNY), which forms cross- β spine structures into a precursor (L-1P) of supramolecular hydrogelator for generating a new precursor L-3P. Our results show that, being dephosphorylated by alkaline phosphatase,

the precursor (L-3P) becomes a hydrogelator (L-3) that self-assembles in water to form nanofibers with an average width 8 ± 2 nm. While the enzymatic formed nanofibers of analogous hydrogelators to display similar morphologies, their precursors exhibit quite different inhibitory activities towards HeLa cells. Our results indicate that the numbers of phenylalanine residues affect the diameters of the nanofibers, the critical strains of the hydrogels, and the ability of the self-assembly of the hydrogelators. Interestingly, the insertion of the amyloid segment into the cytotoxic precursor (D-1P) results in a cell compatible precursor (D-3P), suggesting that the supramolecular arrangement of the hydrogelators in the nanofibers likely play a key role for the cell compatibility of the precursors. This work, thus, not only provides cell compatible hydrogels, but also contributes new insights for the understanding of the biological properties of fibrillar soft nanostructures.

Results and discussion

Schemes 1A and 1B show the molecular design. Based on a known cell compatible precursor of hydrogelator (e.g., N'FFY_p (L-1P), N' = 2-(naphthalen-2-yl)acetic acid),⁴¹ which is a N-terminal capped tripeptide, and a peptide segment (e.g., GNNQQNY (2)) known to form cross- β spine amyloid,¹¹ we design a new precursor (e.g., N'FFGNNQQNY_p (L-3P)) that incorporates the amyloid forming peptide segment (2) and the cell compatible precursor (L-1P). We expect that this straight forward domain insertion of the peptide segment would enhance the self-assembling ability of the cell compatible precursor (or hydrogelators). To evaluate the necessary structural parameters, we also design several structural analogs of L-3P (or L-3). For example, because our previous work shows that phosphatases effectively dephosphorylate D-tyrosine phosphate,³³ we synthesize D-3P (N'ffggnqqny_p), the enantiomer of L-3P, for evaluating the role of D-amino acid in resulting nanoscale assemblies. To examine the role of intermolecular aromatic-aromatic interactions,^{8, 42} we also

^a 415 South Street, MS 015, Waltham, MA 02453, USA. Fax: 781-736-2516; Tel: 781-736-5201; *E-mail: bxu@brandeis.edu.

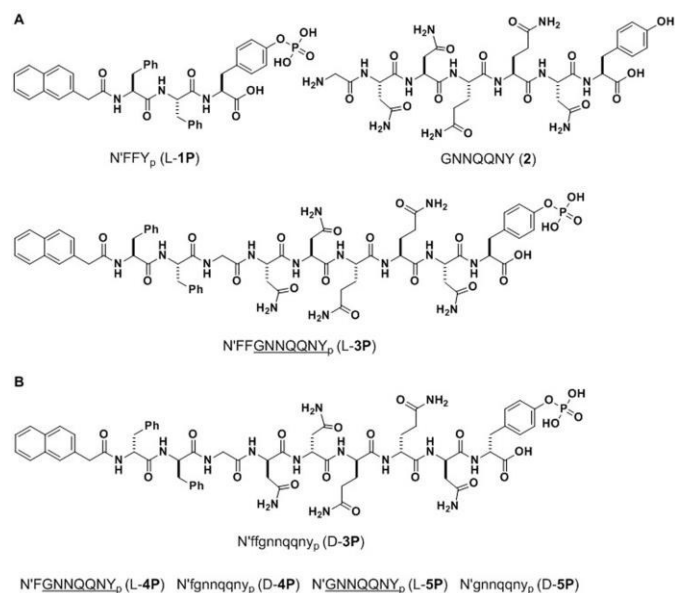
^b Key Laboratory for Molecular Enzymology and Engineering of the Ministry of Education, Jilin University, 2599 Qianjin St., Changchun 130012, China.

†Electronic Supplementary Information (ESI) available: [details of synthesis, NMR, LCMS, TEM, optical images and rheological data]. See DOI: 10.1039/x0xx00000x

ARTICLE

Journal of Materials Chemistry B

reduce the number of phenylalanine residues in L-**3P** (or D-**3P**) to make L-**4P** and L-**5P** (as well as D-**4P** and D-**5P**). We hope that the physicochemical properties and biological activities of L-**3P**, L-**4P**, L-**5P** (or L-**3**, L-**4**, and L-**5**) will reveal the roles of aromatic-aromatic interactions,⁴³ the enzymatic conversion,⁹ and the cross- β spine forming peptide segment¹¹ in the observed behaviours of the resulting nanoscale molecular assemblies.



Scheme 1. (A) The structures of designed precursors and the relevant segments. (B) The structures and peptide sequences of the relevant controls of the molecular amyloids. (N' = the naphthyl acetyl motif. P or p represents the phosphate group. L and D represent the chirality of amino acids in the precursors. For example, L-**3P** converts to L-**3** after dephosphorylation, its enantiomer is D-**3P**).

Solid phase peptide synthesis (SPPS)⁴⁴ provides a facile method for making the precursors. Specifically, we used 2-chlorotrityl chloride resin and *N*-Fmoc amino acids with side chain trityl protecting group. Taking synthesis of L-**3P** as an example, we loaded Fmoc-Tyr(PO₃H₂)-OH^{45, 46} as the first amino acid residue on the resin, followed by sequential addition of Fmoc-Asn(Trt)-OH, Fmoc-Gln(Trt)-OH, Fmoc-Gln(Trt)-OH, Fmoc-Asn(Trt)-OH, Fmoc-Asn(Trt)-OH, Fmoc-Gly-OH, Fmoc-Phe-OH, Fmoc-Phe-OH. After obtain the sequence of FFGNNQQNY_p, we used 2-naphthylacetic acid to cap the *N*-terminal of the peptides. After the deprotection, we used reversed phase high performance liquid chromatography (HPLC) to purify the compound. In a typical run, it is easy to obtain 100 mg of pure compound in timely manner. This rapid synthesis also benefits the production of the analogues of L-**3P** shown in Scheme 1B.

To investigate the properties of L-**3P**, we first checked self-assembly capability of L-**3P** at different pH. While the molecules of L-**3P** (1.1 wt %) self-assemble at pH5 to form nanofibers and to result in a hydrogel (Fig. S4A), the dissolution of L-**3P** (1.5 mg)

in phosphate buffered saline (PBS, 295 μ L) at pH7.4 gives a clear solution. The addition of alkaline phosphatase (ALP) (17 U/mL) to the solution of L-**3P** results in a hydrogel (Fig. 1A, inset) in 10 minutes. This result indicates that the insert of the cross- β forming segment still allows ALP to dephosphorylate the phosphotyrosine residue of L-**3P** in PBS to form L-**3**. As a hydrogelator at pH7.4, L-**3** self-assembles to form a hydrogel. In addition, adjusting pH of the solutions of L-**3P**, L-**4P**, and L-**5P** at the same concentration (1.1 wt %) also can initiate the hydrogelation at pH5, pH4, and pH2, respectively (Fig. S4). These results reveal that decreasing number of phenylalanine in the sequences of the precursors requires more acidic condition for the self-assembly, indicating that the decreased aromatic-aromatic interactions result in the decrease of the ability of the peptides to self-assemble in water. Meanwhile, the enantiomer pair of precursors form hydrogels at the same pH, which is consistent with the behaviours of an enantiomer pair.³⁵ Upon treatment with ALP (17 U/mL), 0.5 wt % of D-**3P**, L-**4P** (or D-**4P**), and L-**5P** (or D-**5P**) all form stable hydrogels. These results confirm that ALP dephosphorylates both the L- and D-phosphotyrosine residues in these enantiomeric precursors that bear the segment of Sup35.

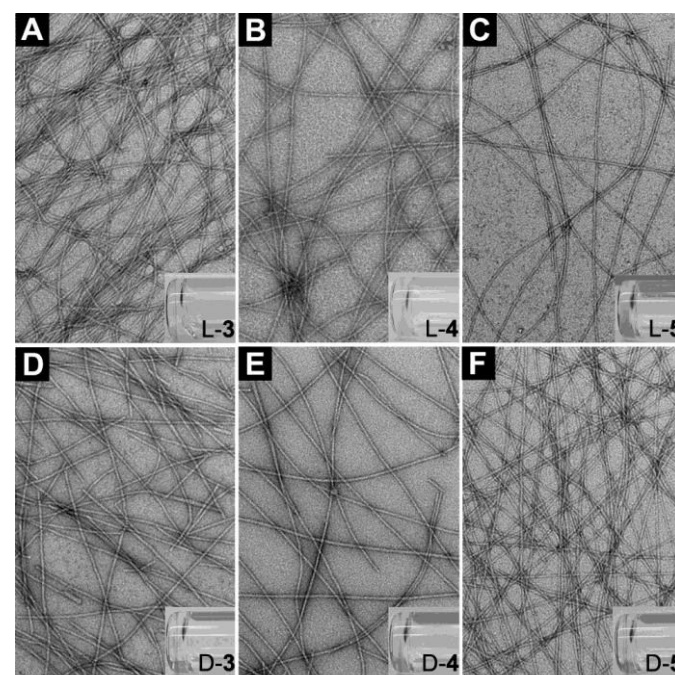


Fig. 1 TEM images and the corresponding optical images of hydrogels formed by (A) L-**3**, (B) L-**4**, (C) L-**5**, (D) D-**3**, (E) D-**4**, and (F) D-**5** after adding ALP in the solutions of the corresponding precursors (L-**3P**, L-**4P**, L-**5P**, D-**3P**, D-**4P**, or D-**5P**) at the concentration of 0.5 wt %, pH = 7.4 in PBS. Scale bar represents 100 nm.

Table 1. Properties of supramolecular nanofibers and hydrogels formed by adding phosphatase or adjust pH of the solutions of precursors.

Precursor	ALP gel ^{a)}			pH gel ^{b)}				IC ₅₀ -48h ^{c)} [μM]
	TEM fiber width [nm]	Dynamic strain sweep		pH	TEM fiber width [nm]	Dynamic strain sweep		
		Critical strains [%]	Max. G' [Pa]			Critical strains [%]	Max. G' [Pa]	
L-3P	8 ± 2	13.2	32.8	5	9 ± 2	4.4	592.5	476.1 ± 21.4***
D-3P	8 ± 2	7.0	132.4	5	9 ± 2	34.4	19.9	>500
L-4P	7 ± 2	6.0	52.2	4	7 ± 2	1.8	69.8	>500
D-4P	7 ± 2	1.6	203.5	4	7 ± 2	1.6	227.2	264.5 ± 28.4**
L-5P	6 ± 2	0.84	205.6	2	8 ± 2	7.3	91.0	>500
D-5P	6 ± 2	0.53	183.7	2	7 ± 2	11.9	41.0	>500

^{a)} ALP gels are the gels of the hydrogelators formed at concentration = 0.5 wt % in PBS, pH = 7.4, by the addition of ALP; ^{b)} pH gels are the gels of the precursors formed at concentration = 1.1 wt %, by adjusting the pH. ^{c)} IC₅₀ of L-1P >500 μM and D-1P = 279 μM³⁵; **2** has poor solubility. **P < 0.01, ***P < 0.001.

We used transmission electron microscopy (TEM) to examine the nanostructure in the hydrogels and used rheometry to assess the viscoelasticity of the hydrogels. As shown in Fig. 1A, the TEM image of hydrogel L-3 consists of long, flexible, and uniform nanofibers with a diameter about 8 ± 2 nm (Fig. 1A). The nanofibers physically entangle together to develop a relative dense network that holds water, which result in a stable hydrogel. The observation of the dense network coincides with the results from the rheological measurement. Fig. 2 shows that the storage moduli (G') of hydrogel L-3 (0.5 wt %) is around 10-fold larger than the corresponding loss moduli (G''), confirming the formation of a viscoelastic hydrogel. Meanwhile, the modulus-strain profile also reveals the critical strain value at which the storage (G') modulus start to decrease significantly due to loss of crosslinking within gel matrix. The critical strain of hydrogel L-3 is 13.2% (Table 1), suggesting that the extensive cross-linking nanofibers is able to resist the deformation of external force. Like L-3P, D-3P also self-assembles to form nanofibers with an average width of 8 ± 2 nm (Fig. 1D). This result agrees well with that the enantiomer pair has similarly physical properties. Like the enantiomer pair of L-3P and D-3P, the enantiomer pair of L-4P and D-4P form uniform nanofibers with width of 7 ± 2 nm (Fig. 1B and Fig. 1E). Additionally, hydrogels of L-5P and D-5P composed by nanofibers with width of 6 ± 2 nm (Fig. 1C and Fig. 1F). Interestingly, the storage moduli of the hydrogels of L-3, L-4, and L-5 are in same magnitude, the critical strains of the hydrogels of L-3, L-4, and L-5 decrease with fewer phenylalanine residues in their sequences, with values of 13.2 %, 6.0 %, and 0.84 %. The largest critical strain in the hydrogel of L-3 likely originates from the high network density of the matrices of the hydrogel. Due to the presence of enzyme, the enzyme triggered hydrogels of L-3 and D-3, as well as other enantiomer pairs, are diastereomeric systems. Thus, it is reasonable to observe the different rheological properties between the hydrogels of L-3 and D-3, with storage modulus 33 Pa and 132 Pa, critical strain 13.2 %

and 7.0 %, respectively. Furthermore, the hydrogels of the precursors formed via pH adjustment also show similar morphological properties, containing long and uniform nanofibers with length of several micrometers (Fig. S4). For example, L-4P and D-4P self-assemble to form nanofibers with width of 7 ± 2 nm. Unlike the hydrogelation triggered by enzyme, the enantiomer pair of pH gels show slightly different morphological (Fig. S4) and rheological properties (Fig. S5, and Table 1), probably caused by the slight difference in the sample preparation.

We also used TEM to evaluate the self-assembly ability of L-3P at concentrations below the gelation concentration in PBS buffer. As shown in Fig. 3, without the treatment of ALP, L-3P also self-assembles to form a few nanofibers and many irregular aggregates even at a concentration of 200 μM (Fig. 3A), nanofiber morphology starts to dominate when the concentrations of L-3P increase to 300 and 500 μM (Fig. 3B and C). After enzymatic dephosphorylation, the resulting L-3 formed uniform nanofibers with an average width about 7 ± 2 nm even at a concentration of 200 μM (Fig. 3E). With the increase of the concentration of solution of L-3, we observed slightly morphological differences in these solutions, which all had long, flexible, and uniform nanofibers with a width about 8 ± 2 nm (Fig. 3F and G). When the concentration increased to 3625 μM (0.5 wt %), L-3P is able to form uniform nanofibers with an average width of 8 ± 2 nm in the absence of ALP, but can't afford a hydrogel (Fig. 3D). The addition of ALP converts the solution to a hydrogel at this condition (Fig. 3H). These results confirm that cleaving of the phosphate group increases the self-assembly ability of the molecules. Together with our previous work that L-1P itself is unable to form nanofibers below 500 μM,⁷ this result confirms that L-3P, resulting from the incorporation of GNNQQN into L-1P, exhibits enhanced self-assembly ability.

Meanwhile, we used MTT assay to evaluate the cellular responses of the resulting peptides. We found that L-3P is

rather cell compatible to HeLa cells⁴⁷, with IC_{50} value of $476.1 \pm 21.4 \mu\text{M}$ at 48 hours (Table 1). This result is consistent with that oligomers of amyloid, rather than their nanofibers and plaques, is the cause of the cytotoxicity.⁴⁸ As the enantiomer of L-3P, D-3P hardly inhibits the proliferation of HeLa cells even at the concentration as high as $500 \mu\text{M}$. With one phenylalanine less than L-3P, L-4P shows the IC_{50} value larger than $500 \mu\text{M}$. Notably, D-4P inhibits HeLa cells ($IC_{50} = 264.5 \pm 28.4 \mu\text{M}$). Like enantiomer pair of L-3P and D-3P, the enantiomer pair of L-5P and D-5P both are cell compatible (IC_{50} value $> 500 \mu\text{M}$).

proteinase K. Based on that only 1.1 % L-4P remains at 1h, and 19.6 % L-3P at 1h, we speculate that the number of phenylalanine also plays a role in the biostability of precursors.

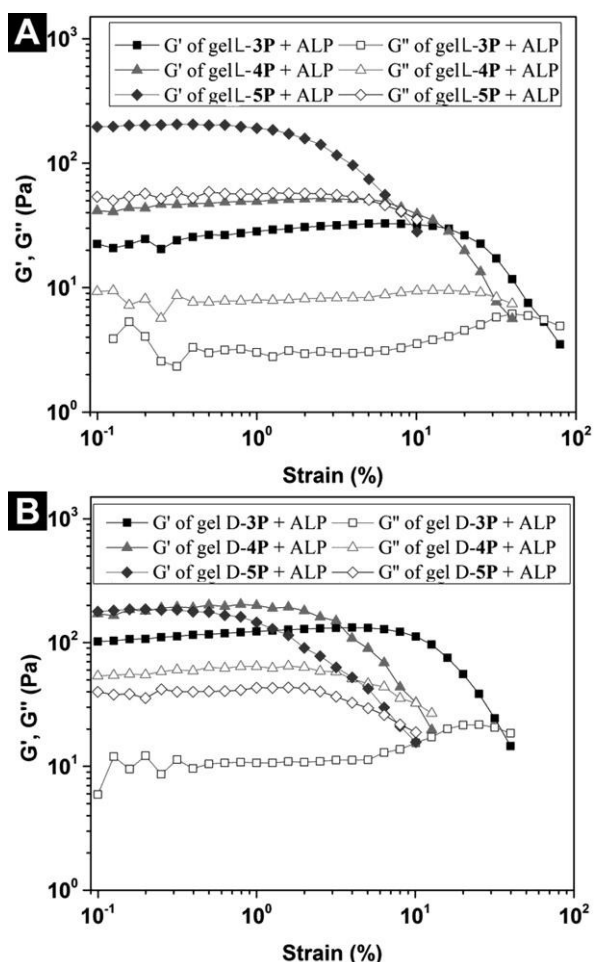


Fig. 2 Strain dependence of the dynamic storage modulus (G') and the loss modulus (G'') of gels shown in Fig. 1 by adding ALP to the solution of the precursors (0.5 wt %) in PBS: (A) L-3P, L-4P, and L-5P; (B) D-3P, D-4P, and D-5P.

Since the existence of proteases in organism catalyzes the hydrolysis of peptide bonds, which affects the stability of peptide-based materials in vivo, we test the proteolytic stability of the precursors containing phenylalanine by incubating them with proteinase K. As shown in Fig. 4, precursors made of D-amino acids, D-3P and D-4P, show high resistance to proteinase K after incubation for 24 h at 37 °C in HEPES buffer. This result agrees with that D-peptide resists proteolytic degradation.⁴⁹ On the contrary, precursors made of L-amino acids, L-3P and L-4P, almost completely degrade after the incubation with proteinase K for 24 h. We only detect the fragment N'F for the degradation of L-3P. While N'F, N'FG and N'FGN coexist as the fragments for the degradation of L-4P at the beginning of incubation with

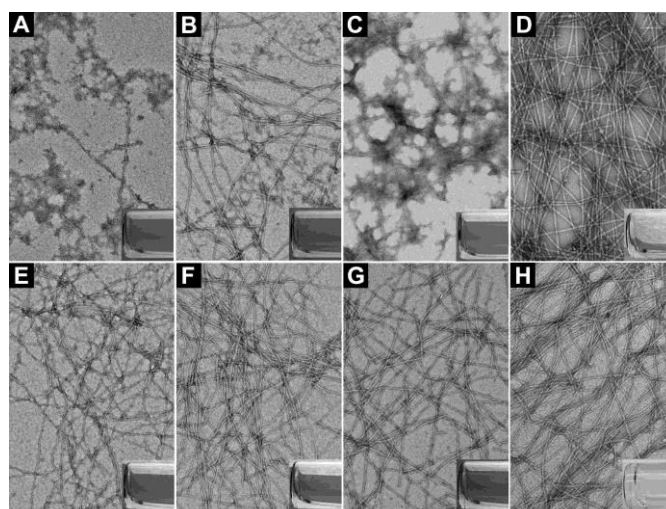


Fig. 3 TEM images of solutions and hydrogel formed by L-3P at different concentrations. The top row solutions are formed by L-3P without the treatment of ALP in PBS: (A) 200 μM , (B) 300 μM , (C) 500 μM , (D) 0.5 wt % (3628 μM). The bottom row solutions and hydrogel are formed by L-3P with the treatment of ALP in PBS: (E) 200 μM , (F) 300 μM , (G) 500 μM , (H) 0.5 wt % (3628 μM). Inserts are the corresponding optical images. Scale bar is 100 nm.

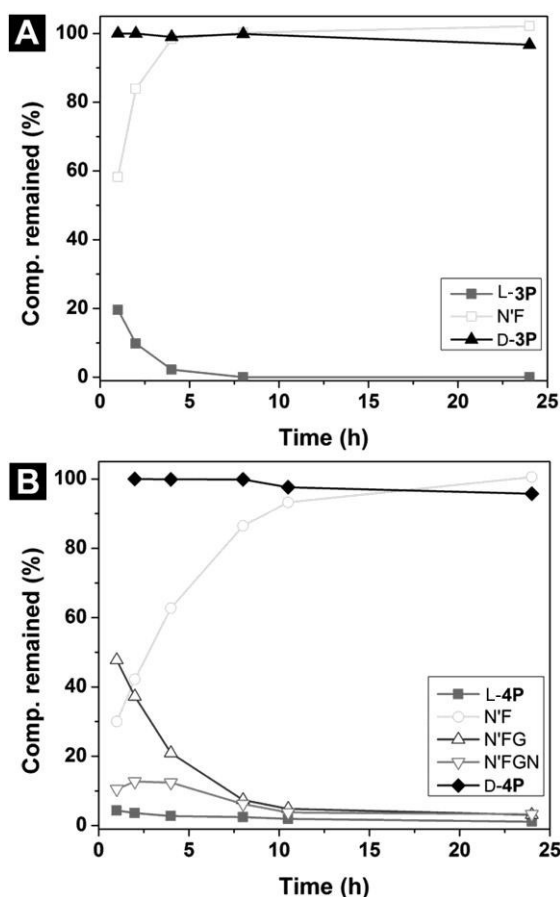


Fig. 4 Time dependent curves of digestion test of (A) L-3P and D-3P, (B) L-4P and D-4P by proteinase K (> 800 U/mL) with the concentration = 0.02 wt % in 10 mM HEPES buffer (4-(2-hydroxyethyl)-1-piperazineethanesulfonic acid). The lines in open symbols are the corresponding fragments of the degradation of L-3P and L-4P.

Conclusions

In conclusion, this work reports that the insertion of amyloid-forming segment into a relative cytotoxic precursor of supramolecular hydrogelator affords cell compatible precursors and hydrogelators. This result implies the simple enhancement of the self-assembly ability may lead to unexpected results. This work, thus, provides a new insight for understanding of cytotoxicity or cell compatibility of nanoscale assemblies of small molecules, a subject⁵⁰ receives less attention but warrants further exploration.

Acknowledgements

This work was partially supported by grant from NIH (CA142746) and Keck Foundation.

Notes and references

- M. C. Branco and J. P. Schneider, *Acta Biomater.*, 2009, **5**, 817-831.
- N. M. Sangeetha and U. Maitra, *Chem. Soc. Rev.*, 2005, **34**, 821-836.

- M. Suzuki and K. Hanabusa, *Chem. Soc. Rev.*, 2009, **38**, 967-975.
- R. V. Ulijn, N. Bibi, V. Jayawarna, P. D. Thornton, S. J. Todd, R. J. Mart, A. M. Smith and J. E. Gough, *Mater. Today*, 2007, **10**, 40-48.
- L. A. Estroff and A. D. Hamilton, *Chem. Rev.*, 2004, **104**, 1201-1217.
- N. A. Peppas, J. Z. Hilt, A. Khademhosseini and R. Langer, *Adv Mater*, 2006, **18**, 1345-1360.
- X. Li, Y. Kuang and B. Xu, *Soft Matter*, 2012, **8**, 2801-2806.
- Y. Zhang, Y. Kuang, Y. Gao and B. Xu, *Langmuir*, 2011, **27**, 529-537.
- Z. Yang, G. Liang and B. Xu, *Acc. Chem. Res.*, 2008, **41**, 315-326.
- H. Su, J. M. Koo and H. Cui, *J. Control. Release*, 2015, **219**, 383-395.
- R. Nelson, M. R. Sawaya, M. Balbirnie, A. O. Madsen, C. Riekel, R. Grothe and D. Eisenberg, *Nature*, 2005, **435**, 773-778.
- M. Balbirnie, R. Grothe and D. S. Eisenberg, *Proc. Natl. Acad. Sci. USA*, 2001, **98**, 2375-2380.
- S. Sur, F. Tantanakitti, J. B. Matson and S. I. Stupp, *Biomater. Sci.*, 2015, **3**, 520-532.
- S. I. Stupp, R. H. Zha, L. C. Palmer, H. Cui and R. Bitton, *Farad. Discuss.*, 2013, **166**, 9-30.
- H. Cui, A. G. Cheetham, E. T. Pashuck and S. I. Stupp, *J. Am. Chem. Soc.*, 2014, **136**, 12461-12468.
- J. P. Schneider, D. J. Pochan, B. Ozbas, K. Rajagopal, L. Pakstis and J. Kretsinger, *J. Am. Chem. Soc.*, 2002, **124**, 15030-15037.
- S. H. Medina, S. Li, O. M. Z. Howard, M. Dunlap, A. Trivett, J. P. Schneider and J. J. Oppenheim, *Biomaterials*, 2015, **53**, 545-553.
- D. M. Ryan, S. B. Anderson and B. L. Nilsson, *Soft Matter*, 2010, **6**, 3220-3231.
- K. Thornton, Y. M. Abul-Haija, N. Hodson and R. V. Ulijn, *Soft Matter*, 2013, **9**, 9430-9439.
- R. A. Pires, Y. M. Abul-Haija, D. S. Costa, R. Novoa-Carballal, R. L. Reis, R. V. Ulijn and I. Pashkuleva, *J. Am. Chem. Soc.*, 2015, **137**, 576-579.
- J. Raeburn, C. Mendoza-Cuenca, B. N. Cattoz, M. A. Little, A. E. Terry, A. Zamith Cardoso, P. C. Griffiths and D. J. Adams, *Soft Matter*, 2015, **11**, 927-935.
- D. Das, S. Maiti, S. Brahmachari and P. K. Das, *Soft Matter*, 2011, **7**, 7291-7303.
- H. Vilaça, A. C. L. Hortelão, E. M. S. Castanheira, M.-J. R. P. Queiroz, L. Hilliou, I. W. Hamley, J. A. Martins and P. M. T. Ferreira, *Biomacromolecules*, 2015, **16**, 3562-3573.
- W. Wang, J. Hu, M. Zheng, L. Zheng, H. Wang and Y. Zhang, *Org. Biomol. Chem.*, 2015, **13**, 11492-11498.
- J. Shi, Y. Gao, Y. Zhang, Y. Pan and B. Xu, *Langmuir*, 2011, **27**, 14425-14431.
- L. Geng, Y. Li, Z. Wang, Y. Wang, G. Feng, X. Pang and X. Yu, *Soft Matter*, 2015, **11**, 8100-8104.
- D. Yuan, X. Du, J. Shi, N. Zhou, J. Zhou and B. Xu, *Angew. Chem. Int. Ed.*, 2015, **54**, 5705-5708.
- D. Yuan, J. Shi, X. Du, N. Zhou and B. Xu, *J. Am. Chem. Soc.*, 2015, **137**, 10092-10095.
- J. Shi, D. Yuan, R. Haburcak, Q. Zhang, C. Zhao, X. Zhang and B. Xu, *Chem. Eur. J.*, 2015, **21**, 18047-18051.
- Y. Zhang, Y. Kuang, Y. A. Gao and B. Xu, *Langmuir*, 2011, **27**, 529-537.
- Y. Gao, J. Shi, D. Yuan and B. Xu, *Nat. Commun.*, 2012, **3**, 1033.
- Y. Kuang, J. Shi, J. Li, D. Yuan, K. A. Alberti, Q. Xu and B. Xu, *Angew. Chem. Int. Ed.*, 2014, **53**, 8104-8107.
- J. Y. Li, Y. Gao, Y. Kuang, J. F. Shi, X. W. Du, J. Zhou, H. M. Wang, Z. M. Yang and B. Xu, *J. Am. Chem. Soc.*, 2013, **135**, 9907-9914.
- J. Shi, X. Du, D. Yuan, R. Haburcak, D. Wu, N. Zhou and B. Xu, *Chem. Commun.*, 2015, **51**, 4899-4901.

ARTICLE

Journal of Materials Chemistry B

- 35 J. Shi, X. Du, D. Yuan, J. Zhou, N. Zhou, Y. Huang and B. Xu, *Biomacromolecules*, 2014, **15**, 3559-3568.
- 36 D. Wu, X. Du, J. Shi, J. Zhou, N. Zhou and B. Xu, *J. Colloid Interface Sci.*, 2015, **447**, 269-272.
- 37 Z. M. Yang, K. M. Xu, Z. F. Guo, Z. H. Guo and B. Xu, *Adv. Mater.*, 2007, **17**, 3152-3156.
- 38 D. Yuan, R. Zhou, J. Shi, X. Du, X. Li and B. Xu, *RCS Adv.*, 2014, **4**, 26487-26490.
- 39 A. Tanaka, Y. Fukuoka, Y. Morimoto, T. Honjo, D. Koda, M. Goto and T. Maruyama, *J. Am. Chem. Soc.*, 2015, **137**, 770-775.
- 40 D. Zhang, G.-B. Qi, Y.-X. Zhao, S.-L. Qiao, C. Yang and H. Wang, *Adv Mater*, 2015, **27**, 6125-6130.
- 41 Z. M. Yang, G. L. Liang, M. L. Ma, Y. Gao and B. Xu, *Small*, 2007, **3**, 558-562.
- 42 J. F. Shi, Y. A. Gao, Z. M. Yang and B. Xu, *Beilstein J. Org. Chem.*, 2011, **7**, 167-172.
- 43 M. L. Ma, Y. Kuang, Y. Gao, Y. Zhang, P. Gao and B. Xu, *J. Am. Chem. Soc.*, 2010, **132**, 2719-2728.
- 44 W. C. Chan and P. D. white, eds., *Fmoc Solid Phase Peptide Synthesis: A Practical Approach*, Oxford University Press Inc., New York, 2000.
- 45 P. F. Alewood, R. B. Johns, R. M. Valerio and B. E. Kemp, *Synthesis-stuttgart*, 1983, 30-31.
- 46 E. A. Ottinger, L. L. Shekels, D. A. Bernlohr and G. Barany, *Biochemistry*, 1993, **32**, 4354-4361.
- 47 J. R. Masters, *Nat. Rev. Cancer*, 2002, **2**, 315-319.
- 48 G. Merlini and V. Bellotti, *N. Engl. J. Med.*, 2003, **349**, 583-596.
- 49 G. Liang, Z. Yang, R. Zhang, L. Li, Y. Fan, Y. Kuang, Y. Gao, T. Wang, W. W. Lu and B. Xu, *Langmuir*, 2009, **25**, 8419-8422.
- 50 J. Shi and B. Xu, *Nano Today*, 2015, **10**, 615-630.

